Influence of Cations, Alkane Chain Length, and Substrate on Molecular Order of Langmuir–Blodgett Films

D. K. Schwartz, R. Viswanathan, J. Garnaes, and J. A. Zasadzinski*

Contribution from the Department of Chemical & Nuclear Engineering, University of California, Santa Barbara, California 93106

Received March 8, 1993

Abstract: Atomic force microscope images of Langmuir–Blodgett films show that manganese arachidate (MnA_2) monolayers are short-range ordered and lead stearate ($PbSt_2$) monolayers are long-range ordered on crystalline mica substrates but disordered on amorphous oxidized silicon substrates. The lattice structures of $PbSt_2$ and MnA_2 monolayers on mica were previously unknown and have larger lattice parameters and molecular areas than do multilayer films of the same materials, indicating the strong interactions with the larger mica lattice. Multilayer films of $PbSt_2$, cadmium arachidate (CdA_2), and MnA_2 have centered rectangular "herringbone" lattices on both silicon and mica substrates. After sufficient layers are added, the effect of the mica substrate is eliminated and the lattice parameters and area per molecule of films deposited on mica relax to those of multilayer films on amorphous oxidized silicon. This limiting area per molecule correlates well with the degree of ionic versus covalent bonding as estimated by the Pauling electronegativity, with barium arachidate (BaA_2) > MnA_2 > CdA_2 > $PbSt_2$. For BaA_2 and MnA_2 the increased molecular area is sufficient to induce a tilt in the molecular packing. The lattice parameters, symmetry, and area per molecule are independent of the length of the alkane chain of the fatty acid for all cations and substrates examined.

Introduction

Because of their applications in the areas of nonlinear optics, molecular electronics, and biosensors,[1] Langmuir–Blodgett (LB) films have been extensively studied by a wide variety of scattering and spectroscopic techniques.[2] Recently, the atomic force microscope[3] (AFM) has emerged as an important tool for studying LB films[4-16] because of its unprecedented ability to measure unaltered films with high lateral resolution and surface selectivity. This permits the observation of not only homogeneous, ordered systems but also defects and inhomogeneities at molecular resolution.[8-16]

In past work we have investigated the prototypic LB system, cadmium arachidate (CdA_2), and have established systematic procedures for quantitative determination of molecular lattice structures and the extent of positional correlation.[10-14] We have attributed the dramatic onset of order between CdA_2 films of 1 and 2 layers to the headgroup–headgroup interaction in these films. In addition, we have observed regular, long-wavelength undulations in the layer thickness[10] that may be related to packing frustration between the polar and nonpolar parts of the fatty acid salt.[17] However, we observed no differences in either the lattice symmetry and dimensions in multilayers or the lack of order in monolayers between films deposited on amorphous oxidized silicon and ordered crystalline mica substrates,[10-14] although there were small differences in the number of macroscopic holes and defects in the films.[14]

These observations motivated us to investigate the effect of incorporating different divalent metal cations and fatty acids of different chain length into films deposited on both amorphous and ordered substrates. Once substrate effects have been accounted for, multilayer Langmuir–Blodgett films of palmitic (P), stearic (St), and arachidic (A) acid salts show that the area per molecule is primarily controlled by the detailed interactions of the counterion with the carboxylic acid group. However, the lattice dimensions and symmetry are dictated by the close packing of the alkane chains, given the constraint of area per molecule set by the counterion. Hence, AFM studies of molecular organization of fatty acid LB films may be ideal systems for checking molecular dynamics calculations of alkane packing.[18] This limiting area per molecule decreases with the degree of ionic versus covalent bonding of the metal ion with the carboxylic acid moiety,[19,20] with barium arachidate (BaA_2) > manganese arachidate (MnA_2) > CdA_2 > lead stearate ($PbSt_2$). For BaA_2[16] and MnA_2 the increased molecular area is sufficient to induce tilt in the molecular packing. The lattice parameters, symmetry, and area per molecule are independent of the length of the alkane chain of the fatty acid (for C_{16} to C_{22}) for all cations and substrates examined.

However, the choice of substrate does have a dramatic effect

* Author to whom correspondence should be addressed: E-mail gorilla@squid.ucsb.edu; FAX 805-893-4731; Phone 805-893-4769.

(1) Roberts, G. G. *Langmuir–Blodgett Films*; Plenum Press: New York, 1990.
(2) Swalen, J. D., et al. *Langmuir* **1987**, *3*, 932–950.
(3) Binnig, G.; Quate, C. F.; Gerber, Ch. *Phys. Rev. Lett.* **1986**, *56*, 930–933.
(4) Marti, O., et al. *Science* **1988**, *239*, 50–53. Egger, M., et al. *J. Struct. Bio.* **1990**, *103*, 89–94. Weisenhorn, A. L., et al. *Langmuir* **1991**, *7*, 8–12.
(5) Meyer, E., et al. *Nature* **1991**, *349*, 398–400.
(6) Hansma, H. G.; Gould, S. A. C.; Hansma, P. K.; Gaub, H. E.; Longo, M. L.; Zasadzinski, J. A. N. *Langmuir* **1991**, 7, 1051–1054.
(7) Zasadzinski, J. A. N.; Helm, C. A.; Longo, M. L.; Weisenhorn, A. L.; Gould, S. A. C.; Hansma, P. K. *Biophys. J.* **1991**, 59, 755–760.
(8) Bourdieu, L.; Silberzan, P.; Chatenay, D. *Phys. Rev. Lett.* **1991**, 67, 2029–2032.
(9) Peltonen, J. P. K.; He, P.; Rosenholm, J. B. *J. Am. Chem. Soc.* **1992**, *114*, 7637–7642.
(10) Garnaes, J.; Schwartz, D. K.; Viswanathan, R.; Zasadzinski, J. A. N. *Nature* **1992**, *357*, 54–57.
(11) Schwartz, D. K.; Garnaes, J.; Viswanathan, R.; Zasadzinski, J. A. N. *Science* **1992**, *257*, 508–511.
(12) Schwartz, D. K.; Garnaes, J.; Viswanathan, R.; Zasadzinski, J. A. N. *Phys. Rev. E* **1993**, *47*, 452–460.
(13) Schwartz, D. K.; Viswanathan, R.; Zasadzinski, J. A. N. *J. Phys. Chem.* **1992**, *96*, 10444–10447.
(14) Viswanathan, R.; Schwartz, D. K.; Garnaes, J.; Zasadzinski, J. A. N. *Langmuir* **1992**, *8*, 1603–1607.
(15) Schwartz, D. K.; Steinberg, S.; Israelachvili, J. N.; Zasadzinski, J. A. N. *Phys. Rev. Lett.* **1992**, *69*, 3354–3357.
(16) Schwartz, D. K.; Viswanathan, R.; Zasadzinski, J. A. N. *Phys. Rev. Lett.* **1993**, *70*, 1267–1270.
(17) Carlson, J. M.; Sethna, J. P. *Phys. Rev. A* **1987**, *36*, 3359–3367. Safran, S. A.; Robbins, M. O.; Garoff, S. *Phys. Rev. A.* **1986**, *33*, 2186–2195. Sadoc, J. F.; Charvolin, J. *J. Phys. (Paris)* **1986**, *47*, 683–690.
(18) Karaborni, S.; Toxvaerd, S.; Olsen, O. H. *J. Chem. Phys.* **1992**, *96*, 4965–4973. Bareman, J. P.; Cardini, G.; Klein, M. L. *Phys. Rev. Lett.* **1988**, *60*, 2152–2155.
(19) Vogel, C.; Corset, J.; Dupeyrat, M. *J. Chim. Phys.* **1979**, *76*, 909–917.
(20) Yazdanian, M.; Yu, H.; Zografi, G. *Langmuir* **1990**, *6*, 1093–1098.

0002-7863/93/1515-7374$04.00/0

on the structure of monolayer and trilayer films for both $PbSt_2$ and MnA_2. Monolayers of $PbSt_2$ deposited on crystalline mica have long-range order while monolayers of MnA_2 on mica show a distinct but short-range order. Otherwise identical lead stearate and manganese arachidate monolayers are completely disordered on amorphous oxidized silicon. Both $PbSt_2$ and MnA_2 monolayers on mica have a significantly larger lattice spacing and molecular area than do the corresponding multilayers on mica, indicating a strong coupling to the mica lattice.[21] For $PbSt_2$ trilayers on mica, the molecular area and lattice parameters were significantly larger than those of $PbSt_2$ trilayers on oxidized silicon.[21] The monolayers of both BaA_2 and CdA_2 were disordered, and for CdA_2 no structural differences were observed between multilayer films deposited on oxidized silicon or mica. (BaA_2 could not be deposited on oxidized silicon.) In addition, the periodic height modulation we have reported for CdA_2[10] changed in wavelength from a value of $\sim$1.9 nm in the case of Cd to $\sim$1.2 nm for Mn. The wavelength of the height modulation is independent of the length of the alkane chain for a given cation, in contradiction to theory.[17] No such height modulation was observed for Pb. BaA_2 films had three distinct lattice arrangements that included much larger height modulations that in turn included stacking faults and offsets by individual methylene units; however, all lattice structures had the same molecular area.[16]

Experimental Section

Behenic ($CH_3(CH_2)_{20}COOH$), arachidic ($CH_3(CH_2)_{18}COOH$), stearic ($CH_3(CH_2)_{16}COOH$), and palmitic acids ($CH_3(CH_2)_{14}COOH$)[22] were spread from chloroform solution (1.7–2.0 mg/mL) onto an aqueous (water from a Milli-Q[23] system was used) subphase in a commercial NIMA Langmuir–Blodgett trough.[24] The cations were added to the subphase as 0.5 mM solutions of $CdCl_2$, $MnCl_2$, $BaCl_2$, or $Pb(CH_3COO)_2$ and the solution pH was adjusted to between 6.5 and 7 (for BaA_2, MnA_2, and CdA_2) by addition of $NaHCO_3$ or to 7.0 ($PbSt_2$) by addition of NaOH ($PbCO_3$ precipitated when we attempted to adjust the pH with $NaHCO_3$). The respective pH's were chosen by using the criterion that the isotherm should contain no trace of the "liquid condensed" phase which exists at lower pH,[6] which correlates well with full complexation of the metal salt.[19,20,25] The only exception is for the alkaline earth metals such as Ba that require significantly higher pH's for full complexation.[19,20] However, BaA_2 multilayers prepared from pH 9.2 showed no difference in macroscopic or microscopic structure with the films prepared at pH 7, which is in agreement with other data in the literature.[16,19] In general, we observed no changes in the structures of any of the films with pH, once the "liquid condensed" phase was absent from the isotherms.[25]

Hydrophilic substrates were freshly cleaved mica or polished silicon wafers[26] (orientation (100), 3 ohm·cm, n-type) with a root-mean-square (rms) roughness of approximately 3 Å as measured by AFM. Prior to deposition, the silicon wafers were cleaned in a hot solution of H_2O_2/H_2SO_4 (3:7 ratio) to remove any organic contaminants while leaving the amorphous native oxide intact and then stored in clean water until use. The mica substrates were cleaned by continuous rinsing with ethanol for 5 min. After removal from the ethanol bath, the mica was cleaved using ordinary adhesive tape and inserted into the subphase. Since all films were Y type (i.e. adjacent layers stack head to head or tail to tail), films deposited on hydrophilic substrates and imaged in air had an odd number of layers (1, 3, 5, 7) with the methyl end of the alkyl chain at the interface. Isotherms and film deposition were done on the Nima[24] trough at 22.0 ± 0.5 °C and a surface pressure of $\pi = 30 \pm 0.1$ dyn/cm. The area per molecule for all species at this surface pressure was in the range of 18–20 Å^2/molecule; there was no correlation between the area per molecule on the trough (relative error ±5%) and the structures we observed on the transferred films.[10,11,16] Film transfer was accomplished by vertical dipping at a speed of approximately 1.6 mm/min. Transfer ratios were approximately unity. Films to be imaged in air (methyl end exposed) were stored in closed containers for times ranging between 1 and 30 days before imaging. The length of time between deposition and imaging did not affect the images.

AFM measurements were performed with a Nanoscope II or Nanoscope III[27] FM in air at room temperature, using a 1 μm × 1 μm scan head and a silicon nitride tip on a cantilever with a spring constant of 0.12 N/m. The best molecular resolution was achieved by using the so-called "force mode", i.e. scanning the tip at approximately constant height and measuring spring deflection. Typical repulsive forces used were on the order of 10 nN. The degree of drift in the image was evaluated by comparing Fourier transforms of images scanned in opposite directions (up and down). The initial variations between spot positions from up and down scans were often as large as 0.03 nm in amplitude and 3° in angle. However, after scanning times on a single area ranging from 0.5 to 2 h, Fourier spots from the two scan directions were in the same location within our ability to measure them given the digitization of the data on the display (0.01 nm, 0.8°). There was no damage done to the samples even after hours of continuous imaging in the AFM.

Statistical analysis similar to that which we have previously reported[12] was used to determine the best quantitative fit to the reciprocal lattice vectors (rlv), $\mathbf{b}_n$, from the Fourier transforms. In principle, the reciprocal lattice vectors could be determined by recording the length and angular orientation of the two linearly independent reflections nearest the origin from the Fourier transform of each image. In practice, however, all of the available reflections are used to provide a best fit lattice structure.[12] The values of the Bravais or real space lattice basis vectors, $\mathbf{a}_1$ and $\mathbf{a}_2$, are calculated from the reciprocal basis vectors $\mathbf{b}_1$ and $\mathbf{b}_2$ by the formulas ($\hat{\mathbf{z}}$ is a unit vector in the direction out of the plane of the Fourier transform):

$$\mathbf{a}_1 = \frac{2\pi \mathbf{b}_2 \times \hat{\mathbf{z}}}{\mathbf{b}_1 \cdot (\mathbf{b}_2 \times \hat{\mathbf{z}})}, \qquad \mathbf{a}_2 = \frac{2\pi \hat{\mathbf{z}} \times \mathbf{b}_1}{\mathbf{b}_2 \cdot (\hat{\mathbf{z}} \times \mathbf{b}_1)}$$

For the rectangular lattices we observe for $PbSt_2$, CdA_2, and MnA_2, $\mathbf{b}_1$ and $\mathbf{b}_2$ are perpendicular to each other, hence

$$a_1 = \frac{2\pi}{b_1}, a_2 = \frac{2\pi}{b_2}$$

in which a_n and b_n are the magnitudes of the Bravais and reciprocal lattice vectors. The molecular area of the unit cell is given by $|\mathbf{a}_1 \times \mathbf{a}_2| = a_1 a_2 \sin\theta$, where θ is the angle between the lattice vectors. Dividing by the number of molecules per unit cell (2 for the rectangular unit cell observed for CdA_2, MnA_2, and $PbSt_2$, 3 and 4 for the two types of BaA_2 lattice) gives the area per molecule listed in Table I. Tilt angles were evaluated by measuring the thickness of the films and by comparing the observed lattice structures with those predicted theoretically by Kitaigorodskii.[31]

In order to calibrate the x and y (lateral) dimensions, 6 images of areas from 30 to 40 nm on a side were obtained from different regions (within 100 nm of each other) on a mica surface. This procedure was repeated with 6 different AFM tips (36 images in total). As the tip is impossible to characterize in detail at the molecular level, we use this procedure to eliminate any systematic errors due to tip shape or any effects of a particular cantilever. For each tip, the reciprocal lattice vectors (rlv), $\mathbf{b}_n$, determined from Fourier transforms, were averaged to reduce statistical fluctuations. The resulting wavevectors were parametrized by the magnitude, a_n, of the Bravais lattice vectors and the angle between adjacent rlv's, $\theta_{n,n+1}$. The six data sets were fit to find the best overall linear calibration constants in x and y directions. The standard deviations from the expected values for mica of $\theta_{n,n+1} = 60°$ and $a_n = 0.450$ nm (adjusted with the best fit calibration) were $\sigma_\theta = 0.9°$ and $\sigma_a = 0.005$ nm. These numbers gave us a guideline as to the degree of reproducibility we could expect from tip to tip on the LB films. It also allowed us to estimate the absolute precision of our m independent calibrations to be $\sigma_a/m^{1/2}a_n = 0.005/[(6^{1/2})0.450] \approx 0.5\%$.[12] Most tips that showed six Fourier spots of relatively equal intensity when imaging mica could be used to image the Langmuir–Blodgett films. (A fraction of tips could not resolve the mica lattice. A more common problem was that a tip would produce

(21) Viswanathan, R.; Schwartz, D. K.; Zasadzinski, J. A. N. Strained-Layer van der Waals Epitaxy in a Langmuir–Blodgett Film. *Science*, in press.

(22) All of the chemicals used in this study were of the highest available purity. Behenic acid, arachidic acid (eicosanoic acid), stearic acid, and sodium bicarbonate were purchased from Aldrich Chemical Co., Milwaukee, WI. Cadmium chloride, manganese chloride, and lead acetate were purchased from Sigma Chemical Co., St. Louis, MO. Spectranalyzed chloroform was purchased from Fisher Scientific, Santa Clara, CA.

(23) Millipore Corporation, Bedford, MA.

(24) NIMA Technology Ltd., Warwick Science Park, Coventry CV4 7EZ, England.

(25) Kobayashi, K.; Takaoka, K.; Ochiai, S. *Thin Solid Films* **1988**, *159*, 267–273. Binks, B. P. *Adv. Colloid Interface Sci.* **1991**, *34*, 343–432.

(26) Semiconductor Processing, Boston, MA.

(27) Digital Instruments, Inc., Goleta, CA 93117.

(28) Bolbach, G., et al. *Thin Solid Films*. **1992**, *210/211*, 524–526.

(29) J. Daillant, et al. *Langmuir* **1991**, *7*, 611–615.

(30) Leveiller, F., et al. *Science* **1991**, *252*, 1532–1536.

(31) Kitaigorodskii, A. I. *Organic Chemical Crystallography*; Consultants Bureau: New York, 1961.

Table I. The Lattice Parameters for LB Films with a Rectangular Two Molecule Unit Cell (Fig. 2), Except Where Noted[a]

material	layers	substrate	a_1 (nm)	a_2 (nm)	molecular area (Å^2)[b]	tilt angle (deg)	corr[c] length (nm)	modulation period (nm)[d]
$PbSt_2$	1	mica	0.447 ± 0.006	0.922 ± 0.008	20.6	0	>40	none
$PbSt_2$	3	mica	0.514 ± 0.006	0.752 ± 0.008	19.3	0	>40	none
$PbSt_2$	5	mica	0.497 ± 0.006	0.739 ± 0.008	18.4	0	>40	none
$PbSt_2$	7	mica	0.493 ± 0.006	0.728 ± 0.008	17.9	0	>40	none
$PbSt_2$	3	silicon	0.492 ± 0.006	0.728 ± 0.008	17.9	0	>40	none
$PbSt_2$	1	silicon	none	none	?	?	?	none
CdA_2	1	mica	none	none	19.4[e]	?	0	none
CdA_2	3	mica	0.482 ± 0.006	0.748 ± 0.008	18.0	0	>40	1.9 ± 0.3
CdA_2	3	silicon	0.482 ± 0.006	0.748 ± 0.008	18.0	0	>40	1.9 ± 0.3
MnA_2	1	mica	0.46 ± 0.01	0.87 ± 0.02	20.0	?	~3	none
MnA_2	3	mica	0.495 ± 0.006	0.791 ± 0.008	19.6	19	>40	1.18 ± 0.08
MnA_2	5	mica	0.481 ± 0.01	0.812 ± 0.01	19.5	19	>40	1.18 ± 0.08
MnA_2	3	silicon	0.477 ± 0.006	0.834 ± 0.008	19.9	19	>40	1.18 ± 0.08
MnA_2	1	silicon	none	none	none	?	0	none
BaA_2	1	mica	none	none	none	?	0	none
BaA_2 (1)	3	mica	0.44 ± 0.01	1.52 ± 0.01	20.4	26	>40	none
BaA_2 (1)	3	mica	0.94 ± 0.01	0.94 ± 0.01	20.2	19	>40	none

[a] For BaA_2, the angle between lattice vectors is 66° for both structures, $\theta = 66°$, and the unit cell for BaA_2 (1) has 3 molecules and that for BaA_2 (2) 4 molecules. [b] The molecular area is given by $a_1 a_2 \sin\theta$/(number of molecules in the unit cell). The tilt angle is measured from the normal to the substrate. [c] The positional correlation length measured along the principal directions of the lattice. [d] The period of the height modulation, if any.[10] [e] Dimensions from electron diffraction which show a hexagonal lattice with short-range order.[12]

molecularly resolved images, but the Fourier pattern was asymmetric and certain pairs of spots were missing. These tips were discarded.)

Results

Parts b, d, and f in Figure 1 show high-resolution images of monolayer LB films of CdA_2, MnA_2, and $PbSt_2$ on mica, respectively, along with their Fourier transforms inset. Figure 1h shows a monolayer film of $PbSt_2$ on oxidized silicon. The CdA_2 and BaA_2 monolayers on mica and all monolayers on silicon appear disordered to the eye, and the Fourier transforms corroborate this. The $PbSt_2$ and MnA_2 monolayers on mica, however, show long-range order in orientation or position or both. In both cases, the lattice is centered rectangular (see Table I); however, there is a qualitatively different lattice symmetry than in the 3-layer films (see Figure 1a,c,e,g).

Each alkyl chain in the 3-layer films of $PbSt_2$ has 4 nearest neighbors at a relatively "close-packed" distance of 0.44–0.45 nm and 2 nearest neighbors at a distance of 0.48–0.51 nm. However, the alkyl chains in the monolayer films have only 2 nearest neighbors at a short distance of 0.45–0.46 nm and 4 nearest neighbors at a distance of 0.49–0.51. This is a previously unreported sort of packing which does not correspond to any of the familiar types of alkane packing that are observed in all other ordered LB films we have imaged,[10–16] although it may be related to a rectangular arrangement based on the "M" packing (which Kitaigorodskii rejects because of its low density) which has "ideal" cell dimensions of $a_1 = 0.42$ nm $a_2 = 0.91$ nm.[31] The nearest neighbor packing in the mica lattice is 0.52 nm, which indicates that the monolayer lattice is most likely expanding to match that of the mica.

Parts a, c, and e of Figure 1 show molecular resolution images of 3-layer LB films of CdA_2, MnA_2, and $PbSt_2$ deposited on mica, respectively, along with their two-dimensional Fourier transforms (FT) inset. Figure 1g shows molecular resolution images of a 3-layer film of $PbSt_2$ deposited on oxidized silicon. Qualitatively, the lattice structure of these 4 films are the same, as the FT's show a rectangular lattice with alternating bright and dim spots. In the cases of CdA_2 and MnA_2 there are additional spots corresponding to a periodic height modulation. As has been previously reported,[10–12] this "diffraction" pattern describes a nearly centered rectangular lattice. The small but finite intensity of the dim Fourier spots (small arrows) is explicit proof that the unit cell consists of two molecules. (The dim spots are the locations of the reciprocal lattice vectors $\mathbf{b}_1$ and $\mathbf{b}_2$.) Because the unit cell contains 2 molecules, and given the particular cell dimensions measured, we conclude that the structure corresponds to a "herringbone" packing called the "R" subcell by Kitaigorodskii.[31]

Figure 2 shows the unit cell deduced from the images, and the dimensions for each material are summarized in Table I. Both CdA_2 and $PbSt_2$ are similar to the "ideal" untilted cell dimensions of $a_1 = 0.496$ nm and $a_2 = 0.742$ nm. However, it is clear that the $PbSt_2$ lattice on mica is significantly larger than that on silicon, indicating a coupling of the mica lattice to the $PbSt_2$ lattice that extends over at least 3 layers. As shown in Table I, however, by layer number 7 the $PbSt_2$ lattice on mica has relaxed to the same dimensions as the 3-layer film on silicon. This limiting molecular area and its associated lattice parameters are very similar to those observed for bulk (>100 layers thick) crystals of $PbSt_2$ as measured by X-ray diffraction.[32–34] Hence, even for mica, the effects of the substrate are eliminated by 7 layers. The MnA_2 lattice is close to the "ideal" tilted (19° in the a_2 direction) cell dimensions of $a_1 = 0.496$ nm and $a_2 = 0.785$ nm.[31] This "ideal" tilt of 19° is based on the idea that alkyl chains prefer to tilt at certain specific angles such that the chain packing in the plane perpendicular to the chains is undisturbed.[31]

Figure 3 shows the structures observed in 3-layer BaA_2 films deposited on mica. (We were unable to deposit BaA_2 films on silicon.)[16] Monolayers of BaA_2 on mica were disordered, suggesting, as for CdA_2,[10–12] that the substrate has a minimal effect on the lattice structure. As described more fully elsewhere,[16] the predominant structure (~70% of the surface area) in Ba arachidate (BaA_2) is a previously unknown lattice best described as a tilted, triclinic packing with a regular commensurate superstructure of packing defects resulting in a "sawtooth" surface modulation and a 3-molecule unit cell of area 61.1 Å^2 (20.4 Å^2/molecule). The effect of the packing defects is to reduce the overall tilt of the triclinic packing from 36° to 26°, thereby decreasing the area per molecule by 4%. The minority structure (<10%) is a 4-molecule unit cell of area 80.7 Å^2 (20.2 Å^2/molecule) in which pairs of molecules are packed in a tilted (19°) rectangular herringbone lattice, but adjacent pairs alternate vertically up and down by a single methylene group. The difference in molecular area between the two lattices is <1%, although the details of the packing arrangement are completely different. The third structure occupies 20–30% of the film area and is untilted but relatively disordered, but it still presents diffuse spots in the Fourier transforms and is close to the same area per molecule as the lattice structures.

Figure 4 shows comparative correlation functions (along a lattice direction) for 1- and 3-layer films of CdA_2, MnA_2, and

(32) Pomerantz, M.; Dacol, F. H.; Segmuller, A. *Phys. Rev. Lett.* **1978**, *40*, 246–249.
(33) Stephens, J. F.; Tuck-Lee, C. *J. Appl. Crystallogr.* **1969**, 2, 1–10.
(34) Prakash, M.; Peng, J. B.; Ketterson, J. B.; Dutta, P. *Chem. Phys. Lett.* **1986**, *128*, 354–357.

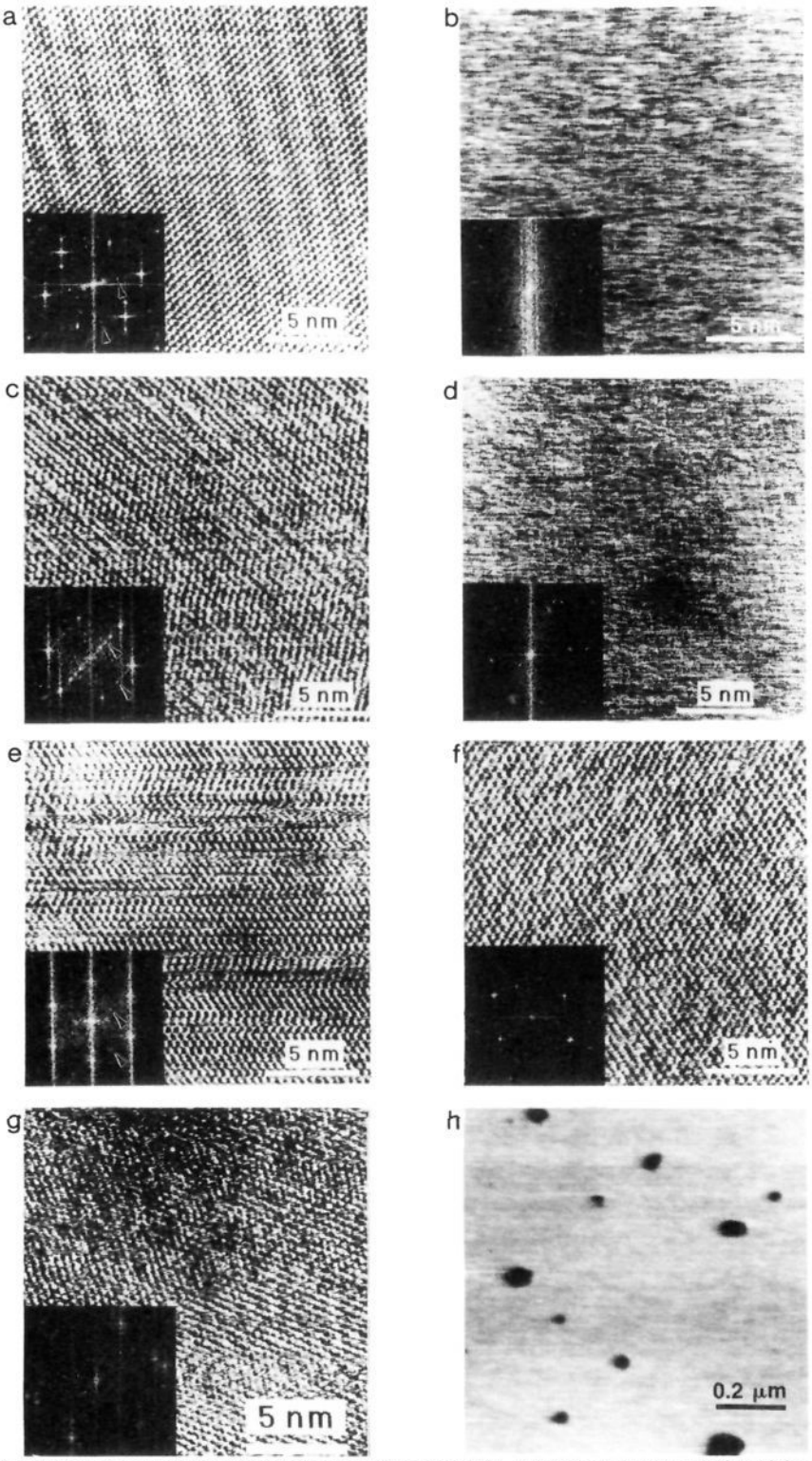

Figure 1. Unprocessed 20 nm × 20 nm images of LB films of various fatty acid salts. Lighter colors correspond to higher areas; the peak to valley height modulation is ~0.2 nm. The respective two-dimensional Fourier transforms are inset. The vertical and horizontal streaks in the FT's are the result of noise from the raster pattern of the AFM. (a) 3-layer CdA_2 on mica—the FT (inset) shows the rectangular reciprocal lattice (arrows). The two inner spots (in the nearly horizontal direction) correspond to the periodic height modulation which is visible as light and dark stripes in the image. (b) 1-layer CdA_2 on mica—the surface is disordered. (c) 3-layer MnA_2 on mica—the Fourier transform inset shows the rectangular lattice (arrows) as well as spots corresponding to the periodic height modulation with a period of about 1.2 nm. (d) 1-layer MnA_2 on mica—the faint lattice structure and broad spots in the Fourier transform are characteristic of the short-range order in this monolayer. (e) 3-layer $PbSt_2$ on mica. The arrows again show the rectangular reciprocal lattice. (f) 1-layer $PbSt_2$ on mica—a molecular lattice is clearly visible. The clear image and spots in the Fourier transform show that this monolayer has a well-ordered lattice. (g) 3-layer $PbSt_2$ on oxidized silicon. The image contains at least two domains of different orientation, likely twinned,[10] and the FT shows the superimposed lattices of the two domains. (h) 1-layer $PbSt_2$ on silicon—no order is visible in the image; the dark spots are monolayer holes in the film.

$PbSt_2$, respectively. The correlations for all of the 3-layer films (solid lines) are hardly diminished at a distance of 10 nm. The monolayer of $PbSt_2$ has similar positional correlations. However, the correlations of the monolayer of MnA_2, although it has

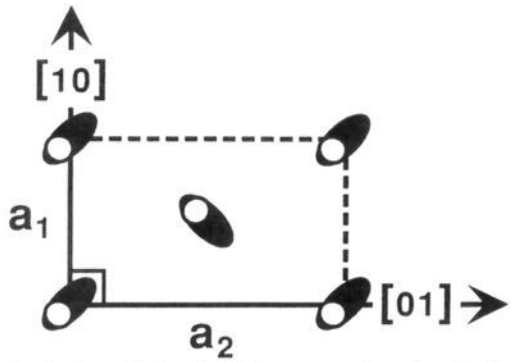

Figure 2. A schematic drawing of the rectangular unit cell. The long axis of the ovals represents the zigzag plane of the alkyl chain. The white circles represent the position of the terminal methyl group. Since every other row has an alternate molecular orientation, the terminal methyl group of the central molecule is not exactly centered in the rectangle formed by the other four methyl groups. Therefore, the unit cell must be described as nearly centered rectangular and contains 2 molecules. Table I summarizes the values of a_1 and a_2.

distinguishable correlation maxima for 5 or 6 repeat distances, dies out by 3 nm. The positional correlation length for the CdA_2 monolayer is less than one repeat distance as demonstrated by the fact that it has no second maximum.

We have previously observed a periodic buckling superstructure along the [01] direction on cadmium fatty acid salt films (see Figure 1a).[10-12] A typical peak to valley height was ≤0.1 nm. We have found the buckling superstructure along the same specific lattice symmetry direction on every film with cadmium counterion we examined for fatty acids of chain length C_{16} to C_{20}. Our measurements also confirmed our earlier findings on CdA_2, that the buckling was independent of the substrate, the surface pressure on the subphase (10–30 mN/m), deposition speed, and the deposition direction. In 45 independent repetitions of the measurement, buckling was present in 30 of the sampled domains. We define a domain to be a continuous area of the LB film with the same lattice structure and orientation, without any evidence of twinning or grain boundaries.[10] Some measurements showed only a "broadband" buckling, i.e. two or more spots with wavelengths from 1 to 3 nm in the [10] direction. However, in

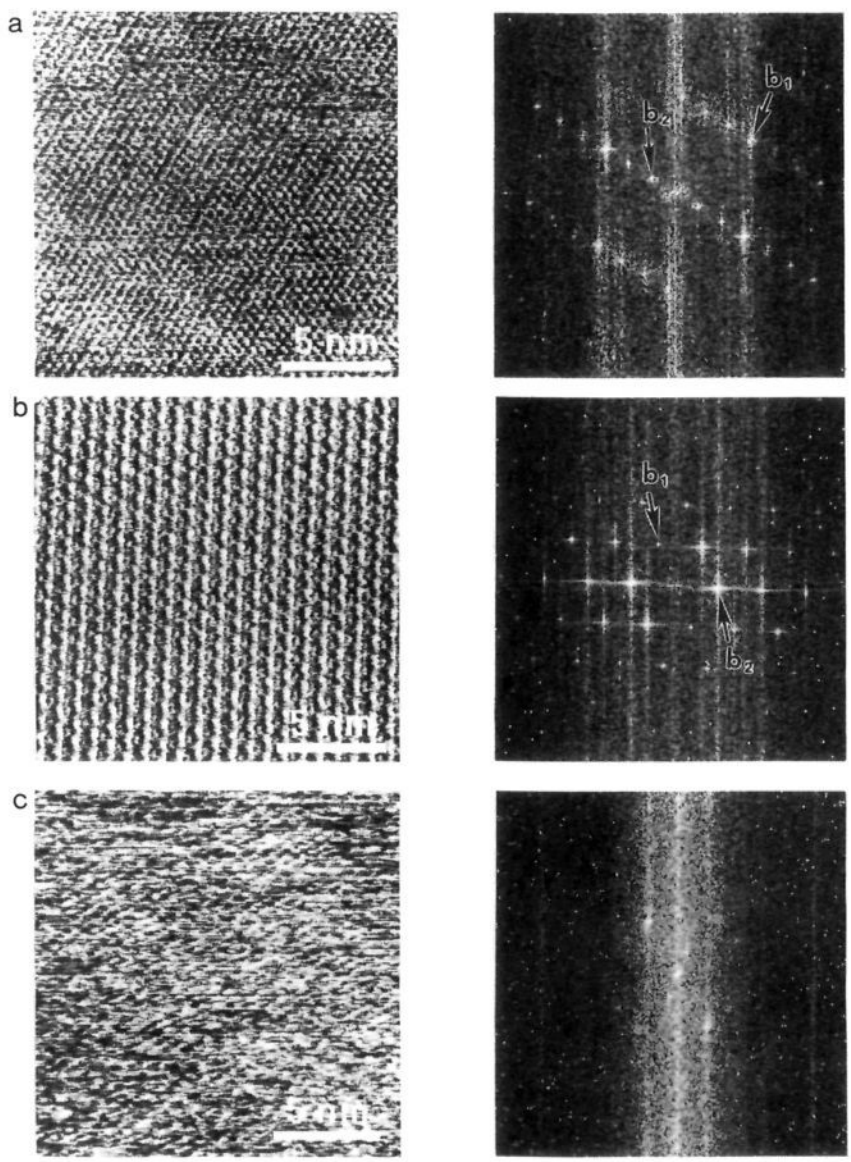

Figure 3. Unprocessed molecular resolution images (left) and Fourier transforms (right) of the three lattice structures seen in BaA_2 films. (a) Lattice 1—a "sawtooth" superstructure is seen every 3 rows. The Fourier transforms (FT) show the basis of the reciprocal lattice labeled. (b) Lattice 2—Alternating rows of high and low zigzag molecules can be clearly seen. (c) Disordered isolated areas of molecular order are visible but without long-range correlation. The FT inset shows that the peaks are diffuse due to short-range order. In all of the FT's, the vertical and horizontal streaks are due to noise generated by the discrete raster pattern of the AFM.

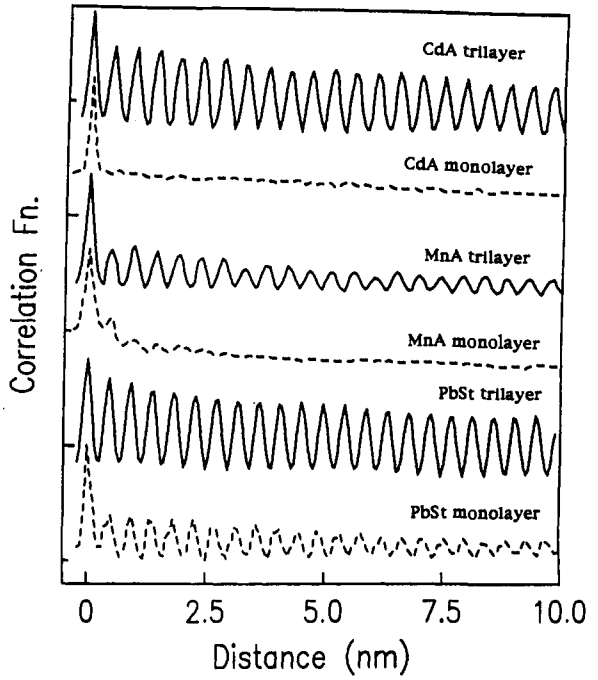

Figure 4. One-dimensional cross sections taken along a lattice direction (when one exists) of the 2-dimensional autocorrelation functions of the images in Figures 1a–f. From top to bottom the data correspond to 3-layer CdA_2, 1-layer CdA_2, 3-layer MnA_2, 1-layer MnA_2, 3-layer $PbSt_2$, and 1-layer $PbSt_2$. The solid lines, corresponding to the 3-layer films, show substantial correlations at 10 nm, as does the dashed line corresponding to the 1-layer $PbSt_2$ film. However, the 1-layer MnA_2 has only 5 or 6 maxima because of its short-range order, and the 1-layer CdA_2 has a correlation length less than the nearest-neighbor distance.

about 60% of the domains with buckling, areas with only one distinct period were identified.

Figure 5 shows the measured period for the buckling superstructure on LB films with hydrocarbon chain lengths of C_{16} (cadmium palmitate), C_{18} (cadmium stearate), and C_{20} (cadmium arachidate). Of the 4 domains examined on cadmium behenate (C_{22}), none had buckling with a distinct period. The average period for the buckling is about 3 unit cells along the [01] direction, corresponding to 2.25 nm. The lattice parameters did not change with alkane chain length over the range examined. For CdA_2, the period of the buckling varied significantly, often even within the same domain. The standard deviation for an individual measurement of the buckling period was 0.09 ± 0.02 nm (small bar on Figure 5). However, the measured buckling periods in different domains have a distribution with a standard deviation of 0.38 ± 0.04 nm. Thus, the variance in the buckling is apparently due to a true distribution of periods with an average of 1.9 nm. A similar analysis of the relative angle of the buckling shows that it is along the [10] direction within about 1°, which is close to our measurement error.

The variance was significantly less for cadmium stearate and cadmium palmitate, which showed a much narrower distribution of buckling wavelengths, much closer to the measurement error. However, the average wavelength of the buckling was identical with that of CdA_2. Theoretical predictions suggest that, if the buckling is due to a frustration in packing incommensurate headgroups and tailgroups, the wavelength should increase with increasing chain length for a given headgroup.[17] What we see is quite different; the variance of the buckling increases with increasing chain length for palmitate to arachidate; however, the average wavelength does not change. The buckling then disappears for behenate. The theories, however, assume a continuous distribution of allowed tilt angles,[17] whereas the preferred alkane packing has distinct preferences for angles that preserve the close packing of the chains.[31] The theories also assume no preferred direction for the buckling; we observe the buckling always occurs along the [01] or next-nearest-neighbor direction.

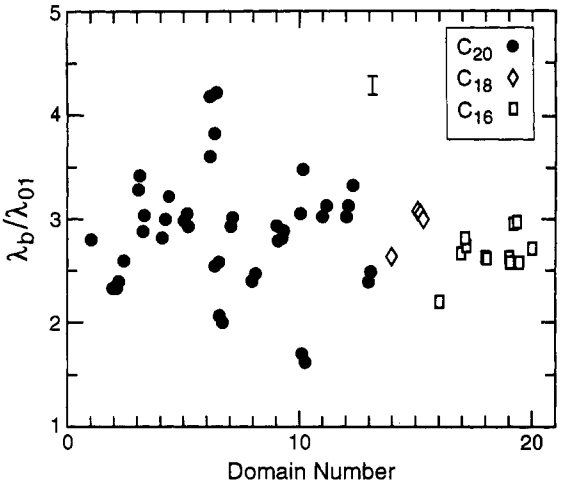

Figure 5. Measured period for the buckling superstructure on cadmium fatty acid salt LB films with hydrocarbon chain lengths of C_{16}, C_{18}, and C_{20}. Each point represents a different measurement on one of the 21 sampled domains. λ_b/λ_{01} is the ratio between the length of the (two molecular) unit cell in the [01] direction and the period of the buckling superstructure. The error bar is two times the standard deviation for a single measurement from the same scan area. The average wavelength of the buckling does not change with chain length, but the variance in buckling period does. No buckling was observed for the cadmium salt of the C_{22} fatty acid.

In all of our measurements of $PbSt_2$ and lead palmitate we were unable to discern any superstructure. However, the 3-layer films of MnA_2 have a very clear superstructure along the [01] direction which is visible in Figure 1c and manifests itself as the Fourier spots closest to the origin. The period of this buckling was found to be 1.18 ± 0.08 nm, considerably less than that found in the cadmium arachidate films. The period of the buckling on MnA_2 is also much better defined, as the error bars reflect the error involved in the measurement while the error bars on the buckling period of the CdA_2 films reflect the fact that the period varies significantly from region to region.

Discussion

From our data, it is clear that the counterion plays the dominant role in determining the area per molecule in Langmuir–Blodgett monolayers and multilayers. The alkane chains then determine the lattice parameters and symmetry that is compatible with close packing,[31] given the constraint imposed by the counterion. Mica substrates can also influence the lattice structure; however, if present, the influence begins with the first monolayer, which is ordered to a greater or lesser extent, and relaxes after 5–7 layers. The length of the fatty acid chain plays no role in the lattice parameters and symmetry, although it does have a limited effect on the details of the buckling superstructure.

The differences between the limiting lattice parameters for the multilayer films must be due to the influence of the cation even though the packing symmetry is determined by the alkane chain packing. We have found reported values of atomic radii for the bare ions of 0.97 Å for Cd^{2+}, 0.8 Å for Mn^{2+}, 1.2 Å for Pb^{2+}, and 1.34 Å for Ba^{2+}.[35] Although the exact values of these parameters may be debated, it is clear that they are not correlated with the limiting area per molecule in LB multilayers, which is $BaA_2 > MnA_2 > CdA_2 \geq PbSt_2$.

Surface potential measurements[20] suggest that the Ba ion and other alkaline earth metals interact with fatty acids electrostatically by screening negative charges in a nonspecific way, while Cd, Mn, and other transition metals interact more specifically via covalent bonding. The effect of pH on isotherms also shows a similar trend. Both Cd and Mn condense partially ionized

(35) *CRC Handbook of Chemistry and Physics*, 59th ed.; Weast, R. C., Ed.; Chemical Rubber Publishing Co.: Boca Raton, FL, 1978.
(36) Betts, J. J.; Pethica, B. A. *Trans. Faraday Soc.* **1956**, *52*, 1581.

fatty acid monolayers, effectively removing the "liquid condensed" phase in isotherms over a pH range of 6–7, which is consistent with the estimated pK_a of the fatty acid film of about 5.6.[24,25] Analysis of LB films of CdA_2 shows complete saturation of the carboxylic acid with the metal ion occurs at a pH of about 6.5. Pb affects the monolayer at significantly lower pH, with the "liquid condensed" phase in isotherms absent at a pH >4,[20] and complete saturation of the carboxylic acid in LB films at a pH of about 4.5.[25] Ba fatty acid LB films do not fully saturate up to a pH of 8.5.[25] Hence, BaA_2 films are a mixture of protonated and deprotonated fatty acids with Ba over the pH range examined here,[16,19] while cadmium, lead, and manganese form specific complexes with deprotonated fatty acids with a well-defined stoichiometry.[10-16,19-21,27-30] The limiting area per molecule appears to be governed by the tendency for covalent bonding, with larger areas per molecule associated with primarily ionic bonding, in the case of Ba, and smaller areas per molecule associated with covalent bonds, especially for Pb. The simplest correlation is the inverse correspondence between the limiting molecular area of the multilayer films and the Pauling electronegativity of 0.9 for Ba, 1.5 for Mn, 1.7 for Cd, and 1.8 for Pb.[37] We can apparently tailor the area per molecule of the fatty acid chains over the range of 17.9–20.6 Å^2 per molecule simply by altering the type of cation. From our data, it appears that the transition from untilted to tilted alkane chains occurs at an area per molecule between 19.3 (3-layer film of $PbSt_2$ on mica) and 19.6 Å^2 (3-layer film of MnA_2 on mica).

In the case of CdA_2 we previously concluded[10-13] that the headgroup–headgroup interface was necessary to stabilize long-range order. Although this appears to be true with cadmium and barium, it is true to a lesser degree with manganese and appears to be incorrect with lead. Long-range order can also be stabilized by an interaction of the film with a specific substrate. However, even in these cases the particular structure formed by the monolayer films is significantly different and more expanded than the multilayer structure. It is possible that there is a specific interaction between the cations and the negatively charged mica. The lattice structure of the cleavage plane of mica is hexagonal with a nearest-neighbor distance of 0.52 nm. The expanded structure of the monolayer lattices contained 4 out of 6 nearest-neighbor distances in the 0.49–0.51-nm range. We will explore this further in future work by seeking to determine if there is commensurate epitaxy between the films and mica, as well as investigating the influence of other substrates on the lattice parameters.[21] In practice, the best order in LB films might be obtained by coupling the lattice structure of the film to the appropriate substrate lattice in an epitaxial fashion.

(37) Pauling, L. *The Nature of the Chemical Bond*, 3rd ed.; Cornell University Press: Ithaca, NY, 1960; p 43.

We postulated previously[10] that the periodic, undulating structures (buckling) that were observed in CdA_2 and MnA_2 might be related to a frustration in molecular packing due to the internal anisotropy of the molecule.[17] In particular, there may be a competition between the packing of the head and tail groups due to different size or symmetry. Hence, a different mean molecular area (of the headgroup) could result in a different buckling period. Mn has a larger ionic radius than cadmium, which may be the cause of the significantly smaller modulation period. This is complicated, however, by the fact that the superstructure in the case of MnA_2 is an excitation about the equilibrium structure of the tilted phase while in the case of CdA_2 it is a variation from the untilted structure. Certainly, this continues to be an interesting area for investigation. One question, in particular, that is quite interesting is why the chain length of the fatty acid fails to influence the average wavelength of the buckling superstructure as predicted by theory.[17] The theories, however, assume a continuous distribution of allowed tilt angles, whereas the preferred alkane packing has distinct preferences for angles that preserve the close packing of the chains.[31]

Conclusions

Atomic force microscopy can provide the most detailed real and Fourier space information available on the structure of Langmuir–Blodgett films of fatty acid salts. We have demonstrated the effects of different cations and substrates on the lattice structure of 1- and 3-layer LB films of barium, cadmium, manganese, and lead fatty acid salts. Although the 3-layer films of all but BaA_2 have similar packing symmetry, the variation in the unit cell dimensions is related to the degree of covalent bonding between the metal ion and the carboxylic acid group, and to specific interactions with the mica substrate. The structure and extent of positional correlations of the monolayer films are dramatically affected by a change in cation and are related to a strong interaction with the mica substrate. The period of buckling modulation (on the 3-layer cadmium and manganese films) is also altered by a change in cation, but not by a change in the alkane chain length.

Acknowledgment. J.A.N.Z. acknowledges useful discussions with G. Zografi, C. Knobler, and H. Yu on the nature of ionic interactions with fatty acids and continued discussions with Paul Hansma on the applications of probe microscopy. This work was supported by the Office of Naval Research under Grant No. N00014-90-J-1551, the National Science Foundation under Grant No. CTS90-15537 and No. CTS-9212790, the National Institutes of Health under Grant No. GM 47334, and the Donors of the Petroleum Research Fund, administered by the American Chemical Society. We also thank Frank Grunfeld of NIMA Technologies for his assistance with the trough and software.